ORIGINAL PAPER

Investigation on effects of system parameters on transmission depth in underwater wireless optical communication

Sanjay Kumar[1] · Shanthi Prince[1] · G. Santosh Kumar[1]

Abstract

Performance of underwater wireless optical communication (UWOC) with different vertical water channel conditions is experimentally analyzed. Experiment has been carried out by varying temperature and salinity of the vertical water channel. Underwater vertical channel is modeled by obtaining the best fit with the experimental data in terms of received optical power as a function of transmission depth and attenuation. This mathematical model is used to simulate UWOC system in Optisystem software to analyze the performance of UWOC in terms of Q factor and BER. Analysis has been carried out to obtain maximum reachable transmission depth at different data rates for fixed input power and maximum achievable data rate at different input power for fixed transmission depth. Maximum reachable transmission depth is also analyzed for different modulation index of the amplitude modulator. These analyses are carried out for optimal performance parameters such as Q factor (≥ 6) and BER ($\leq 10^{-9}$). Apart from Q factor and BER, performance of the UWOC channel is analyzed through eye diagrams obtained at the receiver of the UWOC system in terms of eye height which reflects the quality of signal. This analysis will be helpful for power budgeting, data rate restriction with transmission depth in different water channel conditions to establish vertical UWOC link.

Keywords Underwater wireless optical communication · Vertical water channel · Transmission depth · Blue laser

1 Introduction

About seventy percent of the earth surface is covered with water, out of which ninety five percent belongs to ocean. Due to resource depletion and global climate change, there has been increasing interest to explore the ocean. Underwater wireless communication (UWC) attracts much attention as it enables the realization of ocean exploring system [1]. Some of the main applications which require UWC include tactical surveillance under water, communications between submarines and ships, oil and gas control maintenance, underwater construction and subsea factories, offshore explorations, pollution and climate change monitoring and oceanography research [2, 3]. Deployment of large number of sophisticated sensors and multiple autonomous underwater vehicles

(AUVs) is required for all aforesaid applications and therefore high data rate is required for information transfer under water. Underwater tethers or fibers can be used to achieve such a high data rates but this may be very resistive, expensive or in some case impractical [4].

Acoustic waves, radio frequency (RF) waves and optical waves are three physical carriers for underwater wireless signals. Out of these, acoustic wave system can be used for long range of communication (up to 1000 km) but due to its narrow modulation bandwidth and high frequency dependent attenuation, its data rate is limited to tens of kbps [2]. RF system has been explored as it provides large bandwidth of several MHz and high data rate up to Mbps in underwater environment, but due to its extremely high attenuation in seawater, transmission distance is limited up to 10 m [2, 5].

Optical system can provide high data rates up to few tens of Gbps as required for various underwater communications [6]. A lot of research works have been carried out for space and terrestrial optical communication links [7–12] but underwater wireless optical communication (UWOC) is more challenging than atmospheric wireless optical communication. This is because of the limited availability of

✉ Shanthi Prince
shanthip@srmist.edu.in

1   Department of Electronics and Communication Engineering, Faculty of Engineering and Technology, SRM Institute of Science and Technology, Kattankulathur 603203, Tamil Nadu, India

aquatic optics, LOS, turbulent media and severe attenuation of optical signal in underwater environment [1]. There is wide range of physical processes which occurs in underwater environments ranging from coastal water to deep ocean which are the significant hurdle for reliable UWOC [2]. However, optical waves provide high data rates [13, 14] but it is highly affected by scattering, temperature variations, dispersion, salinity, air bubbles in the medium, etc. Optical signals are highly attenuated due to severe water absorption at optical frequency and back scattered from suspended particles [15], but for blue-green wavelength of EM spectrum the channel has low attenuation [1]. Even after using blue-green wavelength the communication range is limited up to 100 s of meters for high data rate [2].

To enhance the communication range and improve the performance of UWOC, many analysis and investigations have been carried out and also different techniques have been proposed by various researchers. In [16], Multiple-input multiple-output (MIMO) technique is used to mitigate the channel turbulence—induced fading; bit error rate (BER) performance has also been analyzed for MIMO – UWOC. Performance of MIMO-UWOC system with on–off keying modulation and equal gain or optimal combiner has been studied. Exact and upper bound BER expressions are obtained analytically for both equal gain and optimal combining. Performance improvement of 8 dB at BER of 10^{-9} for 3×1 multiple output single output transmission in a link length of 25 m coastal water has been found in [17]. A weighted Gamma function polynomial has been proposed to model the impulse response of general UWOC-MIMO links to investigate the transmission properties of light beams for underwater communications in [18]. Improvement of 32 dB has been achieved at BER of 10^{-6} by using only a dual—hop propagation in a 90 m clear ocean link in [19]. Authors have analytically evaluated the BER of multi-hop UWOC systems and demonstrated that, alleviating channel impairments, multi-hop transmission can significantly improve the performance of the system and enhance the communication range [20]. A routing algorithm for decode and forward as well as amplify and forward relaying schemes are developed to maximize the end-to-end performance. Numerical results demonstrated that network performance and communication range are enhanced significantly [21]. A theoretical fading model has been introduced which accounts for absorption, scattering and turbulence. Numerical results show that turbulence will boost the average capacity under low SNR and at high SNR; average capacity is reduced [22]. A novel UWOC system which is fully compatible with 10Base—T Ethernet transmission, useful for practical marine experiments has been designed and demonstrated [23].

In this study, a wireless optical communication link has been established for a vertical water channel as beam transmission medium and performance analysis of underwater wireless optical communication (UWOC) is carried out in terms of transmission depth, received optical power and data rate. The organization of the paper is as follows: Sect. 2 discusses the optical characteristics of underwater channel. Section 3 presents the experimental set up for analysis of UWOC with vertical water channel for different channel conditions. The mathematical channel modeling is discussed in Sect. 4. Simulation results of the UWOC system with vertical water channel are presented in Sect. 5. Section 6 concludes the paper.

2 Optical characteristics of underwater channel

As from the literature, it is clear that absorption and scattering property of ocean water affect the signal transmission. Optical property of water depends upon the refractive index of water. Temperature is an important factor which affects the refractive index of water. As we go deeper from the surface of ocean water, the temperature decreases [24]. As the temperature of different layers of ocean is different, the refractive index will be different. So, optical signal propagating through these layers will deviate from its original path due to refraction and dispersion which affects the received optical power.

Refractive index of water increases as salinity of water increases. For different oceanic regions of the world, salinity is different for different layers of ocean [25]. The value of salinity ranges from 34 gm/L to 37 gm/L. As the salinity is different for different layers of ocean, the refractive indices will change layer by layer. The change in optical property of water will alter the behavior of optical signal propagating it thereby resulting in changes in the received power [26].

Therefore, behavior of optical signal transmitted through the vertical water channel is different from the horizontal water channel. Hence, the analysis of underwater wireless optical communication with vertical water channel as transmission medium is also needed.

3 Experimental testbed for analysis of UWOC with vertical water channel

To monitor most of the phenomena in underwater environment, a base station can be established on the ocean's surface. An optical wireless link can be established between base station and underwater devices like submarines, autonomous underwater vehicles, unmanned underwater vehicles, etc. to achieve large bandwidth and high data rate.

An experimental testbed has been established to analyze the behavior of optical signal in terms of received power for vertical water channel with respect to earth's surface.

Testbed consists of different length of PVC pipes filled with tap water and saline water fixed vertically with respect to ground. A continuous wave (CW) laser [27] of wavelength 450 nm is used as transmitter which is fixed at upper end of the water column, a silicon photodetector [28] is placed at the lower end to receive the transmitted signal. Power meter [29] is connected to the photodetector to measure the received power. Schematic of experimental testbed is shown in Fig. 1. Specifications of equipment used in establishing experimental testbed taken from the specification sheet of the corresponding equipment are summarized in Table 1.

A UWOC system for vertical water channel has been established in laboratory environment. With the help of this testbed, we analyze UWOC in terms of received power for a vertical column of tap water as channel at the room temperature of $27^0 C$. The experimental testbed is shown in Fig. 2a. Figure 2b shows the laser beam propagating through the channel.

Received power is measured at different depth of transmission by using different length of PVC pipes filled with tap water. The experiment has been repeated in an experimental pool of dimension 180 cm X 50 cm X 65 cm filled with tap water as shown in Fig. 2c. Figure 3 shows the comparison of received optical power at different transmission depth for developed test bed and experimental pool.
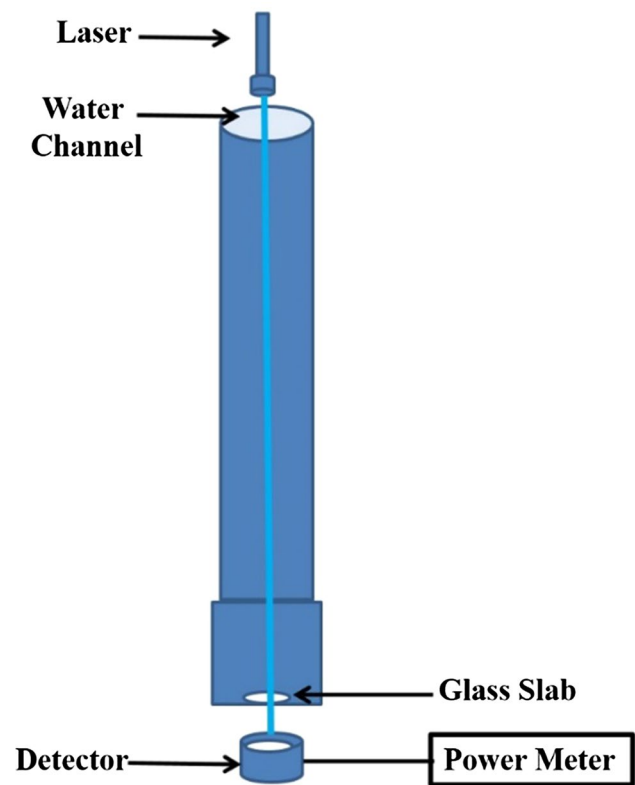

Fig. 1 Schematic of UWOC testbed for a vertical water channel

Table 1 Specifications of experimental testbed equipment

Equipments	Parameters	Values
Laser	Beam diameter (d_{trans})	4.75 mm
	Wavelength	450 nm
	Maximum output power	30 mW
	Output power with water-proof encasing (P_0)	2.145 mW
	Angle of divergence (θ_s)	1.31 milli radians
	Modulation	Up to 100 kHz
Photodetector	Aperture diameter (d_{rec})	10 mm
	Spectral range of detection	420 nm to 1080 nm
	Measurable power	6 nW to 300 mW
	Responsivity	0.45 A/W
Power meter	Power range	4 pW to 30 kW

It can be observed from Fig. 3 that the received power in both the test bed and the experimental pool is almost same and hence the difference in attenuation coefficient (α) will be negligible. Attenuation coefficient being dependent on absorption and scattering coefficient. Vertical channel with PVC pipes which is narrow shows some variation in 'α'. However, as the depth of pool is limited to 65 cm and variation in attenuation coefficient is negligible, experiments have been performed using PVC pipe for longer transmission depth for analysis.

Experiment has also been performed for saline water at room temperature (27° C) with salt concentration of 30 gm/L, 35 g/L and 40 gm/L. Received optical power at different transmission depths obtained from the experiment is plotted in Fig. 4.

It is clear from Fig. 4 that as the transmission depth increases, received optical power decreases for all water channels. The main reason of attenuation of received power is absorption by water channel and scattering due to suspended particles present in the water channel. As the concentration of suspended particles is low in tap water as well as in saline water, the overall attenuation is dominated by absorption. So in this case, absorption is the limiting factor. The concentration of salt present in tap water used in the current experiment is around 0.2 gm/L which is very less as compared to saline water used. Therefore, received power is very less in saline water channel as compared to tap water channel as depicted from Fig. 4. It is also observed from Fig. 4 that as the concentration of saline water is increased, received power decreases. As the attenuation is very high in case of saline water as compared to tap water, the transmission depth is restricted to around 60 cm for saline water channel whereas for tap water, the received power value is decent even at 200 cm.

Fig. 2 **a** UWOC testbed for vertical water channel **b** Laser beam propagating through the vertical water channel in testbed **c** UWOC experimental pool for vertical water channel
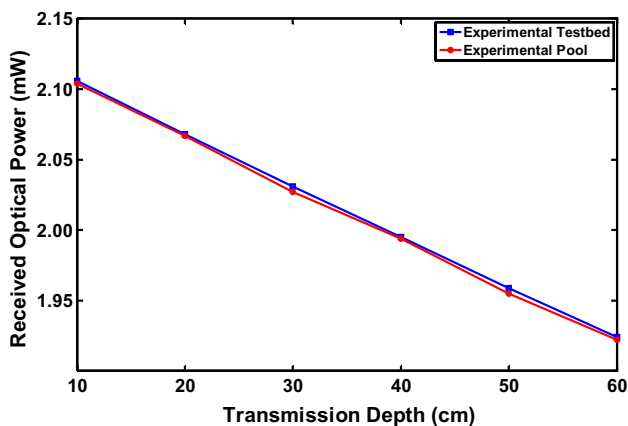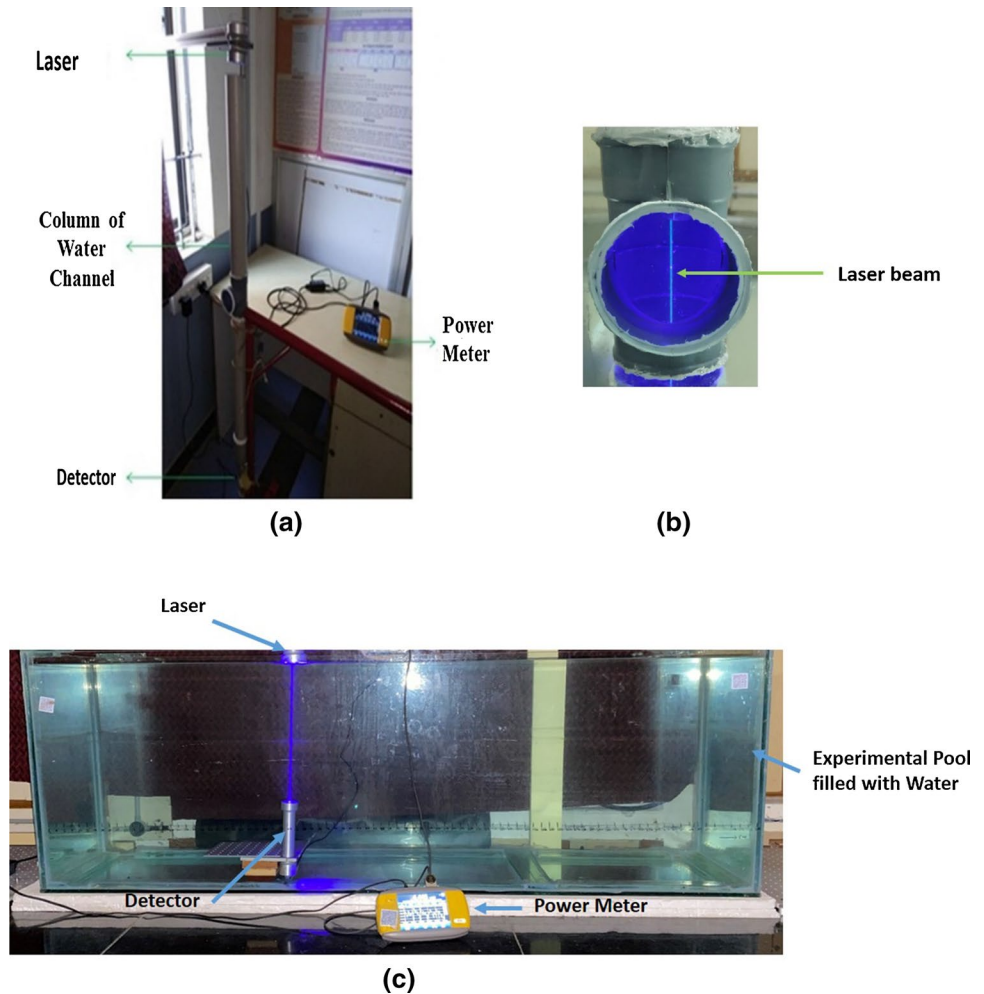

(a)

(b)

(c)

Fig. 3 Comparison of received optical power at different transmission depth for developed test bed and experimental pool

3.1 Analysis of UWOC for a water channel with different salinity level between layers

As could be seen in the literature [30], the salinity of ocean

layers varies with depth. In order to study the variation in the optical signal transmission through different saline layers, an experimental setup with the schematic diagram is shown in Fig. 5. Two columns of water channel are separated by a transparent glass. The lower channel is maintained at fixed salinity value of 34 gm/L, whereas the salinity of upper channel is varied by adding salt using weighing machine.

Received optical power is measured for different values of salinity difference between two layers of water channels which is plotted as shown in Fig. 6. It is clear from figure that as the salinity difference increases, received optical power decreases significantly. Hence, when establishing the vertical optical wireless communication, depending on the ocean layers through which the signal has to traverse, power budgeting need to be done appropriately for successful link establishment.

3.2 Analysis of UOWC for two layers of water layers maintained at different temperature

The temperature of ocean layers varies with depth [24]. In order to study the variation in the optical signal transmission

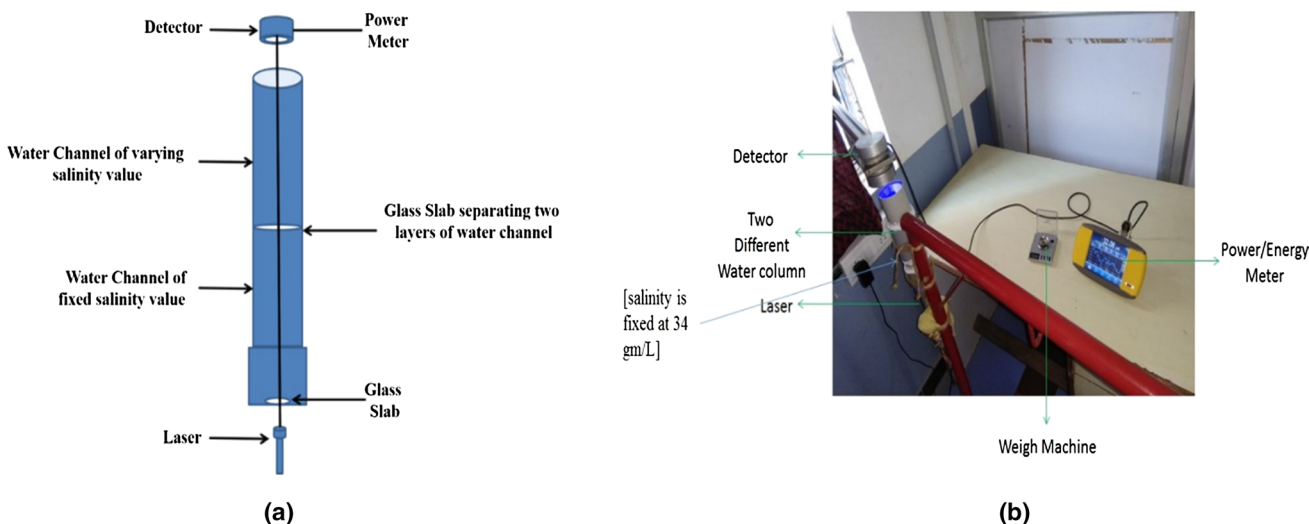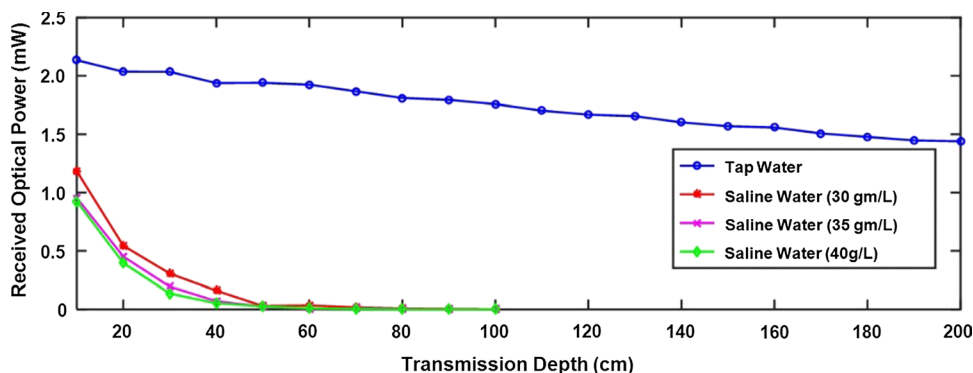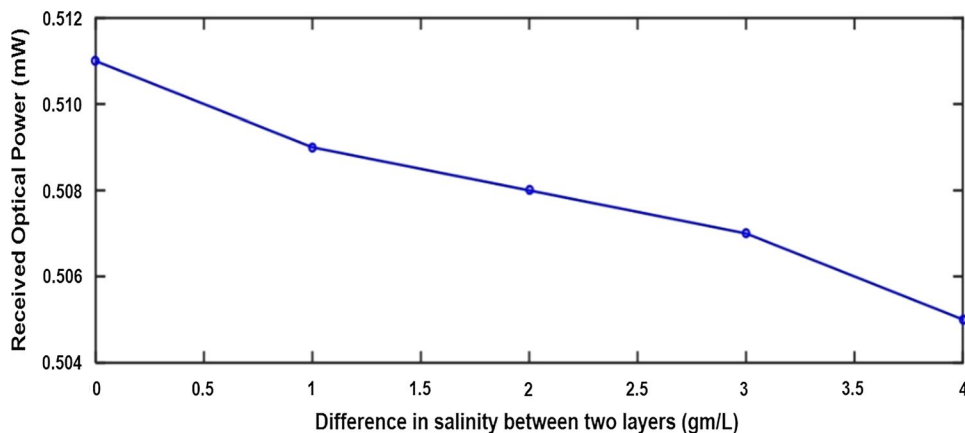**Fig. 4** Variation of received optical power with depth of water channel

Fig. 5 **a** Schematic diagram, **b** Experimental set-up of UOWC for two layers of water channels maintained at different salinity

(a)   (b)

Fig. 6 Received optical power for varying salinity difference between two layers of water channels

through different layers at varying temperature, an experimental setup with the schematic diagram is shown in Fig. 7.

The temperature of lower water channel is fixed at room temperature of 27^0c, whereas temperature of upper water channel has been varied so that the temperature difference between two layers of water channel is varied and for each temperature difference, power has been received at detector end.

Received optical power at different temperature difference between two layers of water channel is plotted as shown in Fig. 8. It is clear from the figure that with
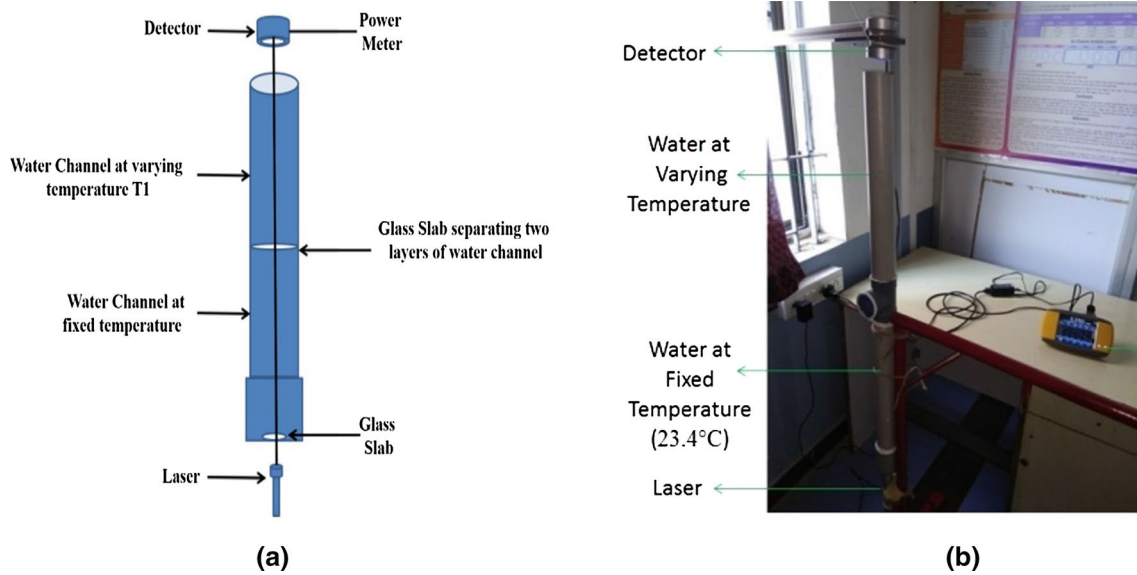
(a)

(b)

Fig. 7 **a** Schematic diagram **b** Experimental setup of UOWC for two layers of water channels maintained at different temperature

increasing temperature difference, the received optical power is decreased significantly.

It is observed from experimental results obtained in Sect. 3.1 and 3.2 that the received power decreases significantly with salinity and temperature difference between layers, resulting in very short range of underwater optical communication link. With proper power budgeting, a vertical optical wireless communication link can be established through ocean layers of different salinity and temperature conditions.

Mathematical modeling is further proposed for homogenous layers of different water channel types for further analysis, using which an UWOC link is simulated and performance is analyzed for different power levels and data rates in terms of BER and Q factor, which are discussed in the followed sections.

4 Mathematical channel modeling

For mathematical modeling of underwater channel, we assume homogenous layer of tap water (comparable with clear ocean water [31]) and saline water with salt concentration of 35 gm/L (salinity comparable with sea bed [30]). Therefore, a mathematical equation is fitted to describe the behavior of UWOC in terms of received optical power for vertical water channel based on the experimental results plotted in Fig. 4. Beer-Lambert's law can be used to analyze the received optical power as function of transmission depth and attenuation [1, 31]. Two assumptions have been considered to use the Beer–Lambert's law for wireless optical communication. First, perfect line-of-sight (LOS) should be maintained between transmitter and receiver. Second, during the propagation of optical signal, the photons which are scattered are lost theoretically but in real-time scenario, some of the scattered photon

Fig. 8 Received power at different temperature difference between two layers
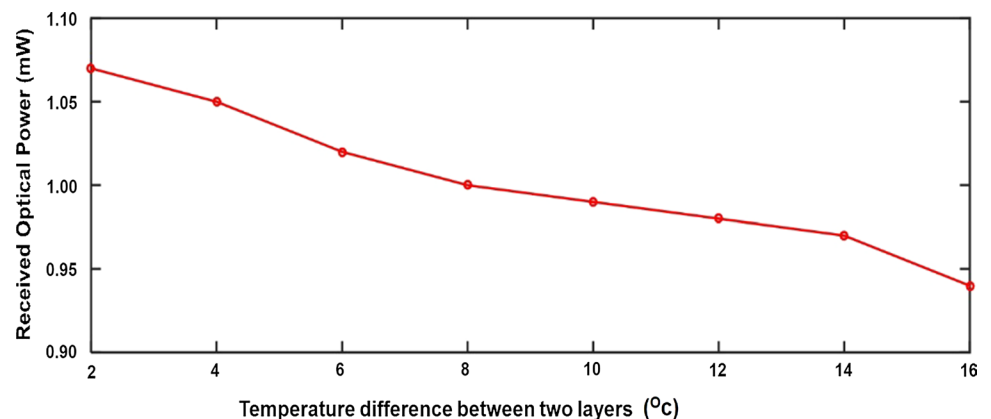
might be received by receiver [1]. In this analysis, experiment has been performed in laboratory environment. Therefore, it is assumed that LOS can be maintained. Also, it is observed during the experiment that received power decreases with increase in channel length which implies that number of photons undergo absorption and scattering increases with channel length. Obtained experimental data have been fitted in a standard mathematical expression which governs Beer–Lambert Law which is given as in Eq. (1).

$$P_{\text{rec}} = P_0 * \exp(-\alpha * h) \tag{1}$$

where P_{rec} is the received optical power at a depth of h, P_0 is the output of laser with waterproof encasing and α is the attenuation coefficient depends on attenuation due to scattering and absorption. The attenuation coefficient 'α' is obtained after fitting the Beer-Lambert's equation as in (1).

Root Mean Square Error (RMSE) which measures the goodness of fit as given by [32] is shown in Eq. (2).

$$\text{RMSE} = \sqrt{\frac{\sum_{i=1}^{n} e_i^2}{n}} \tag{2}$$

where 'n' is the number of samples of error calculated as e_i ($i = 1, 2, 3, …, n$).

Comparison of received optical power at different transmission depth from experiment carried out and analytical values of received power obtained from curve fitting using experimental data is depicted in Fig. 9.

It can be observed from Fig. 9 that experimental and analytical values are almost same. The obtained α value is 0.1806 m^{-1} with RMSE of 0.01877 for tap water, whereas 7.987 m^{-1} with RMSE of 0.01137 for saline water means that Eq. (3) and (4) are the best fit and closely models the experimental data distribution for tap water channel and saline water channel, respectively.

$$P_{\text{rec}} = 2.145 * \exp(-0.1806 * h) \tag{3}$$

$$P_{\text{rec}} = 2.145 * \exp(-7.9870 * h) \tag{4}$$

As optical signal propagates beam diverges resulting in the received beam diameter to be greater than the receiver aperture. Therefore, combined with absorption and scattering loss, beam divergence plays a vital role in signal deterioration. By using a spatial coherent laser source, the beam divergence can be minimized [33]. However, the beam divergence is really determined by the optical channel and the range of communication. For limited range of communication, beam divergence is not significant and therefore Eq. (1) is valid for limited range of communication whereas, beam divergence significantly increases for long range of communication. Therefore, Eq. (1) requires modification for long range of communication.

The fraction the transmitted optical power received at the receiver side due to beam divergence at transmission depth of 'h' can be described by Eq. (5) [33].

$$P_{\text{rec}} = P_0 \left(\frac{d_{\text{rec}}}{d_{\text{trans}} + \theta_s h} \right)^2 \tag{5}$$

where P_0 is the transmitted optical power, d_{trans} and d_{rec} are the diameters of transmitter and receiver aperture. θ_s is the angle of divergence. The values of all these parameters are listed in Table 1.

The generalized mathematical expression governing long range optical communication for long range optical communication can be obtained by combining Eqs. (1) and (5) and is given by Eq. (6).

$$P_{\text{rec}} = P_0 \left(\frac{d_{\text{rec}}}{d_{\text{trans}} + \theta_s h} \right)^2 \exp(-\alpha * h) \tag{6}$$

Equation (6) explicitly accounts for the beam divergence and hence can be considered for long distance communication. Effect of beam divergence can be experienced after a particular minimum communication range and this particular minimum communication range depends upon the transmitter aperture, receiver aperture and angle of divergence. For the current study, Eq. (6) is valid for communication range greater than 4 m.

Fig. 9 Comparison of experimental and analytical fitted values of received optical power
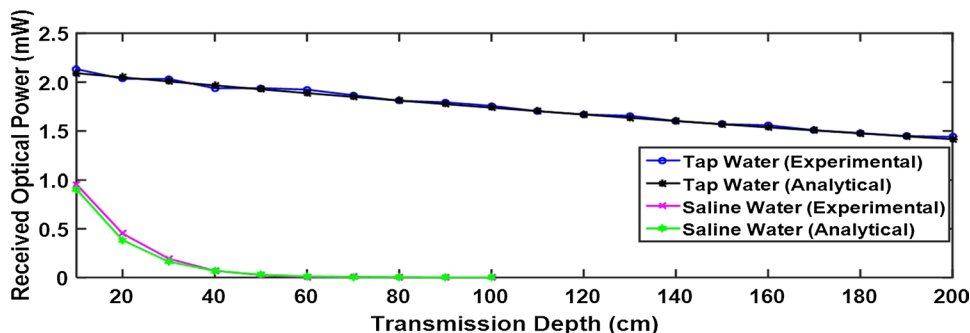
5 Simulation of UWOC system in vertical water channel

In order to analyze the performance of UWOC system with vertical channel for different system parameters such as input power, transmission depth, data rate and modulation index in terms of Q factor and BER, the proposed system is simulated in optisystem (v. 13.0). To simulate the UWOC system, a UWOC vertical channel has been developed in MATLAB using Eq. (5) which models the characteristics of the proposed UWOC channel. The block diagram of UWOC system in optisystem is shown in Fig. 10.

A CW laser of wavelength 450 nm is used as an optical source. The maximum power of the laser which is used in this simulation analysis is 200 mW considering marine life safety [34]. Electrical signal generator generates electrical pulses based on the bit sequence pattern of the pseudo random bit sequence generator. The optical power of CW laser is modulated by the electrical signal in amplitude modulator. The DSB modulated optical signal is then transmitted through the underwater vertical channel. The received signal is detected by a photodetector (PD). The electrical signal, obtained at the output of PD is then analyzed by an electrical signal analyzer. The BER and eye diagram can be analyzed with the help of eye diagram analyzer. Simulation parameters are presented in Table 2.

Different parameters such as input power of CW laser, data rate, transmission depth of the channel, modulation index of the amplitude modulator are varied. The effect of these variations on the UWOC system are analyzed in terms of Q factor and BER for optimal performance of UWOC system with vertical water channel and are discussed in the following sections.

Table 2 Simulation parameters

Parameters	Values
Wavelength of laser	450 nm
Input power of laser	1–200 mW
Input data rate	1 Mbps–5 Gbps
Modulation index of AM	0.1–1
Responsivity of PD	0.45 A/W
Dark current of PD	10 nA
Shot noise of PD	1.56 nA
Thermal noise of PD	31.52 nA

5.1 Impact of transmitted power on transmission depth

The input data rate is fixed at 1 Gbps, modulation index of amplitude modulator is fixed at 1, responsivity of detector is 0.45 A/W and the input power of the CW laser is varied in order to obtain the maximum depth for acceptable BER ($\leq 10^{-9}$) and Q factor (≥ 6) [35–38]. The transmission depth for various input power for tap water channel and saline water channel are presented in Table 3.

It can be observed from Table 3 that when the input power is 1 mW, the reachable transmission depth is 7.7 m for tap water channel, whereas 0.27 m for saline water channel. Similarly, when the input power is increased to 200 mW, the reachable transmission depths are 16.3 m and 0.60 m for tap and saline water channels, respectively. Transmission depth for fixed data rate of 1 Gbps with input power for tap and saline water channels are illustrated in Fig. 11.

It is clear from the slope of the curve in Fig. 11 that as input power increases, the effect of increment in depth of transmission with input power decreases for both the water channel conditions. This is due to the optical property of water, increment in transmission depth follows exponential
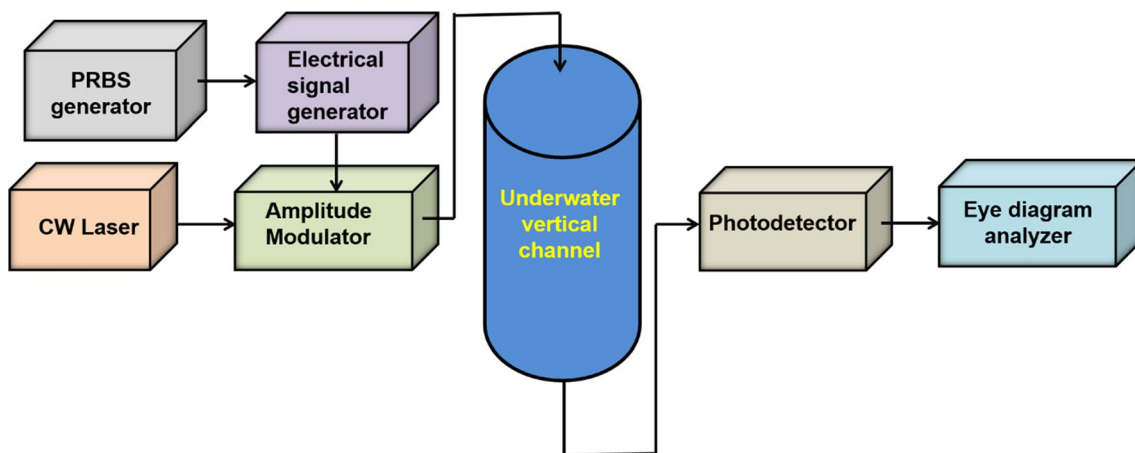

Fig. 10 Block diagram of UWOC system with vertical water channel

Table 3 Maximum transmission depth reachable at different input powers

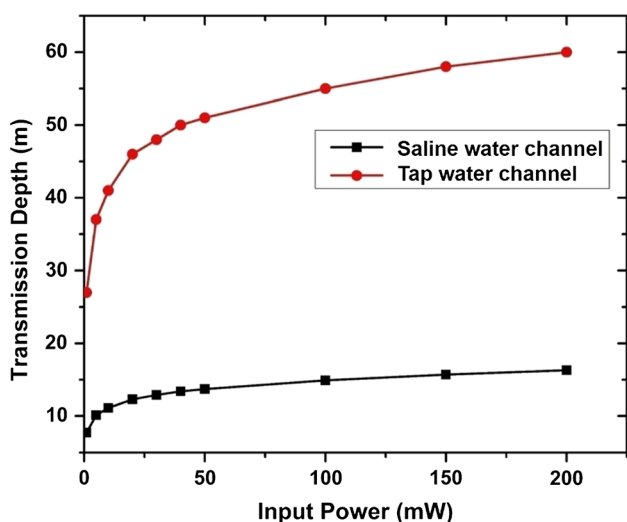| Input power (mW)	Tap water channel			Saline water channel		
	Depth (m)	Q factor	BER	Depth (m)	Q factor	BER
1	7.7	6.23	2.34e−010	0.27	6.15	3.81e−010
5	10.1	6.09	5.57e−010	0.37	6.37	9.42e−011
10	11.1	6.11	4.90e−010	0.41	6.39	7.9e−011
20	12.3	6.05	7.25e−010	0.46	6.28	1.61e−010
30	12.9	6.29	1.53e−010	0.48	6.25	1.99e−010
40	13.4	6.18	3.11e−010	0.50	6.03	8.18e−010
50	13.7	6.23	2.28e−010	0.51	6.68	1.12e−011
100	14.9	6.18	3.16e−010	0.55	6.79	5.47e−012
150	15.7	6.43	6.29e−011	0.58	6.25	1.97e−010
200	16.3	6.11	4.90e−010	0.60	6.15	3.82e−010

Fig. 11 Maximum transmission depth at different input powers for a fixed data rate of 1 Gbps for vertical tap and saline water channels

function. Therefore, as input power increases, the effect of increment in depth of transmission with input power decreases significantly. Thus, it is not always true that efficiency of UWOC can be improved significantly in terms of transmission depth by using a high power laser source.

Figure 12 shows the eye diagram of received signal at a depth of 7.7 m and 16.3 m for a fixed input power of 200 mW for tap water channel.

Eye diagram for saline water channel at a depth of 0.27 m and 0.60 m for input power of 200 mW is shown in Fig. 13.

It is found that eye height at transmission depth of 7.7 m is 5.2e−3 a.u. and the same at 16.3 m is 1.2e−5 a.u for tap water channel. For saline water channel the eye heights are 5.3e−3 a.u. and 1.4e−5 a.u at transmission depth of 0.24 m and 0.60 m, respectively. For a given data rate and input power, the decreased eye height with increased transmission depth affects the quality of received signal as the signal strength deteriorates because of absorption and scattering.

5.2 Impact of data rate on transmission depth

In order to find the maximum reachable depth at varying data rates, the input power is fixed at 200 mW, modulation index at 1 and data rate is varied from 1 Mbps to 5 Gbps. Reachable transmission depth at varying data rate are presented in Table 4. It is observed from Table 4 that as the data rate increases, the maximum reachable transmission depth decreases for a fixed input power in order to obtain acceptable BER and Q factor. This is because as the data rate increases, the identified photodetector is not able to respond to fast changes in signal, resulting in higher error. This leads to decrease in transmission depth. As observed from Table 4, when the data rate is 1 Mbps, the maximum reachable depth for tap water channel is 22.7 m and for saline water channel it is 0.81 m for acceptable Q factor and BER. Similarly, when the data rate is increased to 5 Gbps, the maximum depth that can be achieved for optimal performance is 15 m for tap water and 0.55 m for saline water at fixed input power of 200 mW. Maximum reachable transmission depth at different data rate as recorded in Table 4 is plotted and the resultant graph is shown in Fig. 14.

5.3 Estimation of maximum possible data rate for different input powers

For this analysis, maximum transmission depth of 15 m and 0.55 m are considered for tap water and saline water, respectively. The modulation index of the amplitude modulator and responsivity of the detector are fixed at 1 and 0.45 A/W, respectively. The data rates are optimized at different input powers for acceptable Q factor and BER. Table 5 shows maximum achievable data rates at different input powers for tap water and saline water.

It is clear from Table 5 that maximum achievable data rate at input power of 1 mW is 150 Kbps for tap water and 140 Kbps for saline water, whereas at 200 mW, the maximum
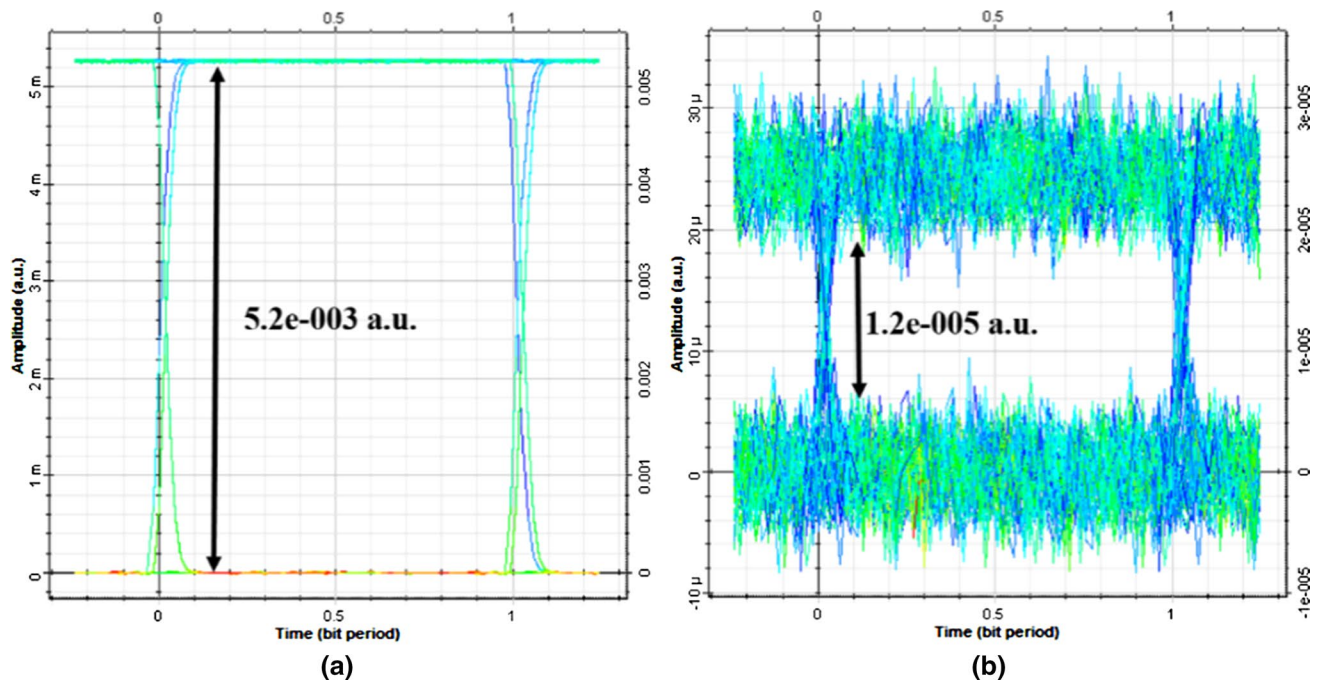
Fig. 12 Eye diagram of the received signal at a depth of **a** 7.7 m **b** 16.3 m at input power of 200 mW for tap water channel
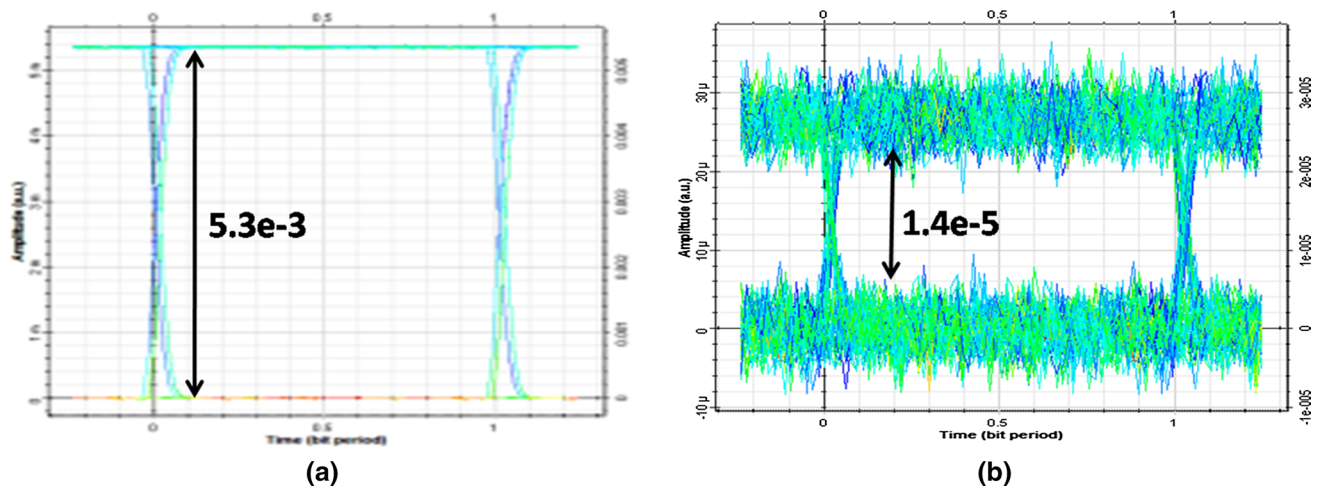

Fig. 13 Eye diagram of the received signal at a depth of (a) 0.27 m (b) 0.60 m at input power of 200 mW for saline water channel water channel

achievable data rate is 5 Gbps for a fixed transmission depth of 15 m for tap water and and 0.55 m transmission depth of saline water, respectively.

5.4 Impact of modulation index of the amplitude modulator on transmission depth

The maximum reachable transmission depth depends upon the modulation index at fixed data rate and input power [39]. The data rate is fixed at 1 Gbps, input power is 200 mW and maximum transmission depth is achieved at different

modulation indices of the amplitude modulator varied from 0.1 to 1 in steps of 0.1 at acceptable Q factor and BER. Maximum transmission depth achieved at different modulation indices for tap water channel and saline water channel is presented in Table 6.

It is observed from Table 6 that maximum reachable transmission depth increases with modulation index. As observed, when the modulation index is 0.1, the maximum transmission depth is 11.9 m and 0.44 m for tap and saline water, respectively, whereas when the modulation index is 1, the maximum transmission depth is 16.3 m and 0.60 m

Table 4 Maximum reachable transmission depth for varying data rate for fixed input power

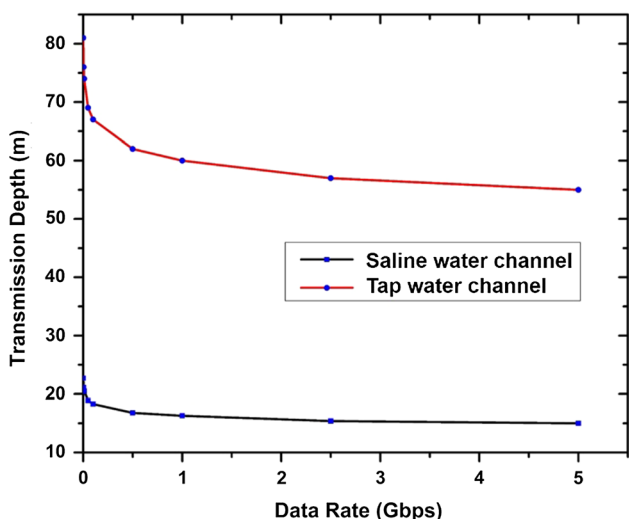| Data rate	Tap water channel			Saline water channel		
	Depth (m)	Q factor	BER	Depth (m)	Q factor	BER
1 Mbps	22.7	6.07	6.39e−010	81	6.95	1.78e−012
5 Mbps	21.1	6.21	2.53e−010	76	6.93	1.96e−012
10 Mbps	20.5	6.02	8.64e−010	74	6.76	6.74e−012
50 Mbps	18.9	6.31	1.42e−010	69	6.74	7.88e−012
100 Mbps	18.3	6.16	3.58e−010	67	6.56	2.64e−011
500 Mbps	16.8	6.00	9.36e−010	62	6.53	3.18e−011
1 Gbps	16.3	6.11	4.89e−010	60	6.15	3.82e−010
2.5 Gbps	15.4	6.07	6.36e−010	57	6.40	7.76e−011
5 Gbps	15	6.04	7.49e−010	55	6.17	3.31e−010

Fig. 14 Maximum transmission depth at varying data rate at a fixed input power of 200 mW for tap water channel and saline water channel

for tap and saline water, respectively. The variation of maximum reachable transmission depth with modulation indices is plotted as shown in Fig. 15.

It can be inferred from Fig. 15 that as the modulation index increases and approaches to unity, the maximum transmission depth also increases.

6 Conclusion

In the current study, experimental and simulation analysis is carried out to observe the impact of transmitted power and data rate on the maximum reachable depth of transmission for different vertical water channel conditions. Based on the experimental data, attenuation coefficient of the water channels under study is obtained by curve fitting, which is later used to model the vertical water channels for simulation. The modeled vertical water channel is then simulated at different data rate, transmission depth, input power and modulation index of amplitude modulator. The performance of UWOC system with vertical water channel is analyzed in terms of Q-factor and BER for the aforementioned parameter variations. It is observed that for tap water channel, when the input power is 200 mW, the maximum reachable transmission depth is 16.3 m for acceptable BER and Q factor at a data rate of 1 Gbps and the maximum reachable transmission depth is reduced to 15 m if data rate is increased to 5 Gbps.

Table 5 Maximum data rate at different input powers for fixed transmission depth of 15 m for tap water and 0.55 m for saline water

Input power (mW)	Tap water channel			Saline water channel		
	Data Rate	Q factor	BER	Data Rate	Q Factor	BER
1	0.15 Mbps	6.00	9.58e−010	0.14 Mbps	6.04	7.36e−010
5	3.7 Mbps	6.04	7.49e−010	3.5 Mbps	6.04	7.40e−010
10	14.8 Mbps	6.00	9.81e−010	14 Mbps	6.04	7.56e−010
20	59.4 Mbps	6.02	8.64e−010	55 Mbps	6.08	5.68e−010
30	131 Mbps	6.07	6.33e−010	120 Mbps	6.15	3.84e−010
40	236 Mbps	6.02	8.70e−010	220 Mbps	6.06	6.47e−010
50	269 Mbps	6.00	9.44e−010	340 Mbps	6.03	7.97e−010
100	1.4 Gbps	6.10	5.02e−010	1 Gbps	6.79	5.47e−012
150	3.2 Gbps	6.00	9.79e−010	3 Gbps	6.03	7.94e−010
200	5 Gbps	6.34	1.14e−010	5 Gbps	6.17	3.31e−010

Table 6 Maximum transmission depth at different modulation indices of the amplitude modulator for tap water channel and saline water channel

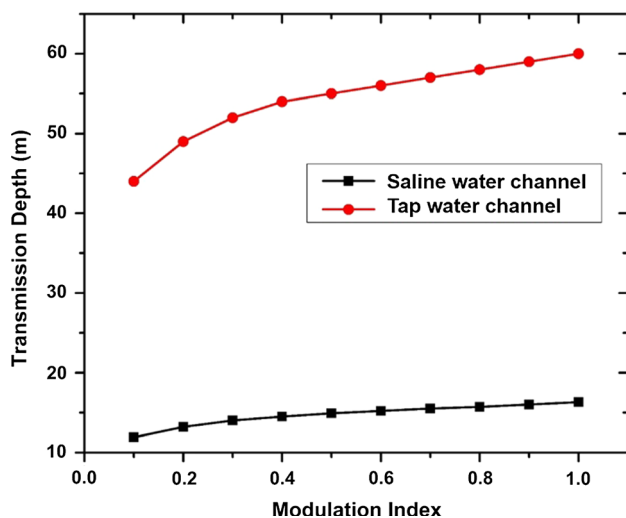| Modulation index	Tap water channel			Saline water channel		
	Depth (m)	Q factor	BER	Depth (m)	Q factor	BER
0.1	11.9	6.16	3.59e−010	0.44	6.26	1.87e−010
0.2	13.2	6.28	1.68e−010	0.49	6.58	2.30e−011
0.3	14	6.04	7.54e−010	0.52	6.24	2.15e−010
0.4	14.5	6.28	1.66e−010	0.54	6.08	5.90e−010
0.5	14.9	6.01	9.08e−010	0.55	6.55	2.86e−011
0.6	15.2	6.38	8.59e−011	0.56	7.02	1.05e−012
0.7	15.5	6.03	7.92e−010	0.57	6.71	9.45e−012
0.8	15.7	6.21	2.60e−010	0.58	6.58	2.24e−011
0.9	16.0	6.00	9.44e−010	0.59	6.95	1.71e−012
1	16.3	6.11	4.89e−010	0.60	6.15	3.82e−010

Fig. 15 Maximum reachable transmission depth at varying modulation indices of the amplitude modulator for tap water channel and saline water channel

Once the channel attenuation is known, the required system can be proposed using the simulation model developed to study the vertical water channel.

As a future scope, the current study can be extended to analyze the performance of UWOC system for vertical water channel medium using different advanced modulation schemes such as QAM, QPSK, and OFDM. Also, this study can be carried out for different water channels such as turbid harbor and coastal ocean water.

Whereas for saline water channel, at a fixed input power of 200 mW, the maximum reachable transmission depth is 0.60 m at 1 Gbps data rate and 0.55 m at 5 Gbps data rate for acceptable BER and Q factor. Therefore for saline water channel, the transmission depth is significantly decreased at fixed power and data rate as compared to saline water channel due to high attenuation of optical signal in saline water. It has also been observed that at higher input power, increment in transmission depth with increment in input power is negligible in any water channel. Therefore, it is not always true that efficiency of UWOC can be improved significantly in terms of transmission depth by using a high power laser source. Another parameter of interest which affects the performance of the UWOC system is modulation index of the amplitude modulator. As, the modulation index increases from 0.1 and approaches unity, the transmission depth is observed to increase for fixed input power and data rate.

References

1. Zeng, Z., Fu, S., Zhang, H., Dong, Y., Cheng, J.: A survey of underwater optical wireless communications. IEEE Commun. Surv. Tutor. **19**(1), 204–238 (2017)
2. Kaushal, H., Kaddoum, G.: Underwater optical wireless communication. IEEE Access **4**, 1518–1547 (2016)
3. Alipour, A., Mir, A.: On the performance of blue–green waves propagation through underwater optical wireless communication system. Photon Netw. Commun. **36**(3), 309–315 (2018)
4. Arvanitakis, G., McKendry, J., Bookey, H.T., Gu, E. and Dawson, M.D.: Light emitting diodes and lasers for high-speed underwater optical communications. Undersea Defence Technology (2018)
5. Al-Halafi, A., Oubei, H.M., Ooi, B.S., Shihada, B.: Real-time video transmission over different underwater wireless optical channels using a directly modulated 520 nm laser diode. IEEE/OSA J. Opt. Commun. Netw. **9**(10), 826–832 (2017)
6. Fu, Y., Du, Y.: Performance of heterodyne differential phase-shift-keying underwater wireless optical communication systems in gamma-gamma-distributed turbulence. Appl. Opt. **57**(9), 2057–2063 (2018)
7. Huang, X., Zhang, J.A., Liu, R.P., Guo, Y.J., Hanzo, L.: Airplane-aided integrated networking for 6G wireless: Will it work? IEEE Veh. Technol. Mag. **14**(3), 84–91 (2019)
8. Pinna, S., Zhao, H., Brunelli, S.Š., Song, B., Sang, F. and Klamkin, J.: High-power integrated indium phosphide transmitter for free-space optical communications. In Proc. of Asia

Communications and Photonics Conference, Chengdu, pp. S3E-5 (2019)

9. Malik, S., Sahu, P.K.: Free space optics/millimeter-wave based vertical and horizontal terrestrial backhaul network for 5G. Opt. Commun. **459**, 125010 (2020)

10. Soni, G.G., Tripathi, A., Mandloi, A., Gupta, S.: Compensating rain induced impairments in terrestrial FSO links using aperture averaging and receiver diversity. Opt. Quant. Electron. **51**(7), 244 (2019)

11. Nistazakis, H.E., Tsiftsis, T.A., Tombras, G.S.: Performance analysis of free-space optical communication systems over atmospheric turbulence channels. IET Commun. **3**(8), 1402–1409 (2009)

12. Nema, S., Oza, S., Parmar, A., Shah, D. and Singh, S.: Implementation of wavelength diversity technique in free-space optical link. In: Proc. of International Conference on Innovations in Electronics and Communication Engineering, Hyderabad, pp. 241–251 (2019)

13. Iyer, S., Singh, S.P.: Spectral and power efficiency investigation in single-and multi-line-rate optical wavelength division multiplexed (WDM) networks. Photon Netw. Commun. **33**(1), 39–51 (2017)

14. Iyer, S. and Singh, S.P.: Investigation of launch power and regenerator placement effect on the design of mixed-line-rate (MLR) optical WDM networks. Photonic Netw. Commun., pp.1–17 (2017)

15. Singh, S.P., Iyer, S., Kar, S., Jain, V.K.: Study on mitigation of transmission impairments and issues and challenges with PLIA-RWA in optical WDM networks. J. Opt. Commun. **33**(2), 83–101 (2012)

16. Jamali, M.V. and Salehi, J.A.: On the BER of multiple-input multiple-output underwater wireless optical communication systems. In: Proc. of 4th International Workshop on Optical Wireless Communications (IWOW), Istanbul, pp. 26–30 (2015)

17. Jamali, M.V., Salehi, J.A., Akhoundi, F.: Performance studies of underwater wireless optical communication systems with spatial diversity: MIMO scheme. IEEE Trans. Commun. **65**(3), 1176–1192 (2017)

18. Zhang, H., Dong, Y.: Impulse response modeling for general underwater wireless optical MIMO links. IEEE Commun. Mag. **54**(2), 56–61 (2016)

19. Jamali, M.V., Akhoundi, F., Salehi, J.A.: Performance characterization of relay-assisted wireless optical CDMA networks in turbulent underwater channel. IEEE Trans. Wireless Commun. **15**(6), 4104–4116 (2016)

20. Jamali, M.V., Chizari, A., Salehi, J.A.: Performance analysis of multi-hop underwater wireless optical communication systems. IEEE Photonics Technol. Lett. **29**(5), 462–465 (2017)

21. Celik, A., Saeed, N., Al-Naffouri, T.Y. and Alouini, M.S., 2018, April. Modeling and performance analysis of multihop underwater optical wireless sensor networks. In 2018 IEEE Wireless Communications and Networking Conference (WCNC) (pp. 1–6). IEEE

22. Zhang, H., Cheng, J., Wang, Z. and Dong, Y., 2018, On the capacity of buoy-based mimo systems for underwater optical wireless links with turbulence. In: 2018 IEEE International Conference on Communications (ICC) (pp. 1–6). IEEE

23. Cossu, G., Sturniolo, A., Messa, A., Scaradozzi, D., Ciaramella, E.: Full-fledged 10Base-T ethernet underwater optical wireless communication system. IEEE J. Sel. Areas Commun. **36**(1), 194–202 (2018)

24. Vedachalam, N., Ramesh, S., Prasanth, P.U., Ramdass, G.A.: Modeling of rising methane bubbles during production leaks from the gas hydrate sites of India. Mar. Georesour. Geotechnol. **36**(8), 966–973 (2018)

25. Liu, C., Liang, X., Ponte, R.M., Vinogradova, N., Wang, O.: Vertical redistribution of salt and layered changes in global ocean salinity. Nat. Commun. **10**(1), 1–8 (2019)

26. Kumar, S., Prince, S., Aravind, J.V., Kumar G. S.: Analysis on the effect of salinity in underwater wireless optical communication. Mar. Georesour. Geotechnol., pp.1–11 (2019)

27. https://www.edmundoptics.com/p/450nm-30mw-h3-blue-laser-diode-module/3333/

28. https://www.edmundoptics.com/p/0420-108mum-300mw-silicon-power-detector/31862/

29. https://www.edmundoptics.com/p/eo-premier-powerenergy-meter/31858/

30. Talley, L.D.: Salinity patterns. In: MacCracken, M.C., Perry, J.S. (eds.) Encyclopedia of Global Environmental Change, pp. 629–640. John Wiley and Sons, Chichester (2002)

31. Wang, J., Lu, C., Li, S., Xu, Z.: 100 m/500 Mbps underwater optical wireless communication using an NRZ-OOK modulated 520 nm laser diode. Opt. Express **27**(9), 12171–12181 (2019)

32. Nguyen, H., Bui, X.N.: Predicting blast-induced air overpressure: a robust artificial intelligence system based on artificial neural networks and random forest. Nat. Resour. Res. **28**(3), 893–907 (2019)

33. Ghassemlooy, Z., Popoola, W., Rajbhandari, S.: Optical Wireless Communications: System and Channel Modelling with Matlab. CRC Press, Florida (2019)

34. http://www.deepsea.com/knowledgebase/technical-resources/diode-lasers-in underwater-applications. Accessed 10 March 2020

35. Sumathi, K., Balasaraswathi, M., Boopathi, C.S., Singh, M., Malhotra, J. and Dhasarathan, V.: Design of 3.84 Tbps hybrid WDM–PDM based inter-satellite optical wireless communication (IsOWC) system using spectral efficient orthogonal modulation scheme. J. Ambient Intell. Humanized Comput., pp.1–9 (2020)

36. Li, C.Y., Lu, H.H., Chen, Y.N., Su, C.W., Wu, Y.R., Wang, Z.H., Lin, Y.P.: A high-speed and long-reach PAM4 optical wireless communication system. IEEE Photonics J. **10**(4), 1–9 (2018)

37. Wu, D., Ghassemlooy, Z., LeMinh, H., Rajbhandari, S. and Kavian, Y.S.: Power distribution and q-factor analysis of diffuse cellular indoor visible light communication systems. In: Proc. of 16th European Conference on Networks and Optical Communications, UK, pp. 28–31 (2011)

38. Chaudhary, S., Tang, X., Sharma, A., Lin, B., Wei, X., Parmar, A.: A cost-effective 100 Gbps SAC-OCDMA–PDM based inter-satellite communication link. Opt. Quant. Electron. **51**(5), 148 (2019)

39. Lian, J., Gao, Y., Wu, P., Lian, D.: Orthogonal frequency division multiplexing techniques comparison for underwater optical wireless communication systems. Sensors **19**(1), 1–19 (2019)

Sanjay Kumar received the B.Sc. Engg. degree in Electronics & Communication Engineering from R.P. Sharma Institute of Technology, Patna, India, in 2010, and the M. Tech degree in Communication Systems from SRM University, Kattankulathur, India, in 2015. He is currently working towards the Ph.D. degree in Optical Communication at SRM Institute of Science and Technology, Kattankulathur, India. His research interest include Underwater Wireless Optical Communication, Underwater Positioning and Navigation, Underwater Sensors, Antenna System and Design.

Shanthi Prince is a Professor in the department of Electronics and Communication Engineering, SRM Institute of Science and Technology. Her research interests include diffuse reflectance spectroscopy studies on tissues, development of non-invasive instrumentation for biomedical applications, underwater optical wireless communication, optical wireless channel modelling, passive optical networks, all optical processing, Visible light communications. She has published several papers in reputed journals and is the author of a book, four book chapters and co-author of three book chapters. She is the recipient of IETE-CEOT award for the contributions in the field of Biophotonics for the year 2016 and the recipient of Dr. A. P. J. Abdul Kalam Inspiring Teacher Award instituted by IET CLN for the year 2014–15. She is currently working on research projects funded by DRDO and ISRO, Government of India.

G. Santosh Kumar received the B.E. degree in Electronics and Communication Engineering from Mahendra Engineering College, Namakkal, India, in 2014, and the M. Tech degree in Communication Systems from SRM University, Kattankulathur, India, in 2016. He is currently working as Junior Support Engineer in Macs Infosolution India Pvt Ltd.